

Biomaterials Science: Processing, Properties and Applications IV

Edited by
Susmita Bose
Amit Bandyopadhyay
Roger Narayan

Ceramic
T*ransactions*
Volume 251

The
American
Ceramic
Society



WILEY

Contents

[Cover](#)

[Half Title page](#)

[Title page](#)

[Copyright page](#)

[Preface](#)

[**Bioactive Glass-Ceramic Scaffolds
with High-Strength for Orthopedic
Applications**](#)

[Introduction](#)

[Methodology](#)

[Results and Discussion](#)

[Conclusions](#)

[Acknowledgments](#)

[References](#)

[**Metallurgical Characterization of
Laser-Sintered Cobalt-Chromium
Dental Alloy**](#)

[Introduction](#)

[Experimental Procedures](#)

[Results](#)

[Discussion](#)
[Conclusions](#)
[Acknowledgment](#)
[References](#)

Mechanical Properties, Microstructures, and Biocompatibility of Low-Cost β -Type Ti-Mn Alloys for Biomedical Applications

[Introduction](#)
[Experimental](#)
[Results and Discussion](#)
[Conclusions](#)
[Acknowledgement](#)
[References](#)

Microstructural Characteristic of Nano Calcium Phosphates Doped with Fluoride and Titanium Ions

[Introduction](#)
[Method](#)
[Results and Discussion](#)
[Conclusions](#)
[References](#)

Development of Implants Composed of Hollow Hydroxyapatite Microspheres for Bone Regeneration

- [1. Introduction](#)
- [2. Creation of Implants Composed of Hollow HA Microspheres](#)
- [3. Hollow HA Microspheres as a Device for Controlled Delivery of BMP2](#)
- [4. In Vivo Performance of Hollow HA Microspheres](#)
- [5. Conclusions](#)
- [References](#)

Porous Titanium Implants Fabricated by a Salt Bath Sintering Process for Bone Repair Applications

- [Introduction](#)
- [Experiment Procedure](#)
- [Results](#)
- [Discussion](#)
- [Conclusion](#)
- [References](#)

Navigating the Uncharted Waters of the New AIA U.S. Patent Law

- [Prior Art Under the New AIA Patent Law](#)
- [Applicant Employer Companies Now Have More Options in Patenting Process](#)
- [Post Grant Review and Inter Partes Review](#)
- [Derivation Proceeding](#)
- [Prior Commercial Use Defense](#)
- [Preissuance Submission](#)
- [Supplemental Examination](#)

[How the New Law is Applied, Using a
Hypothetical Concerning Biomedical Device
Patents](#)
[Practice Tips](#)
[Conclusion](#)
[Disclaimer](#)

Comparative Analysis of Hydroxyapatite and Titanium-Based Bioscaffolds Fabricated Via Adaptive foam Reticulation

[Introduction](#)
[Materials and Methodology](#)
[Results and Discussion](#)
[Conclusions](#)
[Acknowledgements](#)
[References](#)

Laser Processing of Tricalicum Phosphate Reinforced Cobalt - Chrome Alloy Coatings

[Introduction](#)
[Lens™ Processing](#)
[Mechanical Testing](#)
[Results](#)
[Discussion](#)
[Summary](#)
[Acknowledgements](#)
[References](#)

Effect of Degree of Deacetylation of Chitosan on Macrophage Function

[Introduction](#)

[Materials and Methods](#)

[Results and Discussion](#)

[Conclusion](#)

[References](#)

PECVD SiO_x Accelerates Hydroxyapatite Surface Formation for Enhanced Early Osteogenic Differentiation

[Introduction](#)

[Materials and Methods](#)

[Results](#)

[Discussion](#)

[Conclusions](#)

[Acknowledgements](#)

[References](#)

Author Index

Biomaterials Science: Processing, Properties and Applications IV

Biomaterials Science: Processing, Properties and Applications IV

Ceramic Transactions, Volume 251

Edited by
Susmita Bose
Amit Bandyopadhyay
Roger Narayan



WILEY

Copyright © 2014 by The American Ceramic Society. All rights reserved.

Published by John Wiley & Sons, Inc., Hoboken, New Jersey.
Published simultaneously in Canada.

No part of this publication may be reproduced, stored in a retrieval system, or transmitted in any form or by any means, electronic, mechanical, photocopying, recording, scanning, or otherwise, except as permitted under Section 107 or 108 of the 1976 United States Copyright Act, without either the prior written permission of the Publisher, or authorization through payment of the appropriate per-copy fee to the Copyright Clearance Center, Inc., 222 Rosewood Drive, Danvers, MA 01923, (978) 750-8400, fax (978) 750-4470, or on the web at www.copyright.com. Requests to the Publisher for permission should be addressed to the Permissions Department, John Wiley & Sons, Inc., 111 River Street, Hoboken, NJ 07030, (201) 748-6011, fax (201) 748-6008, or online at <http://www.wiley.com/go/permission>.

Limit of Liability/Disclaimer of Warranty: While the publisher and author have used their best efforts in preparing this book, they make no representations or warranties with respect to the accuracy or completeness of the contents of this book and specifically disclaim any implied warranties of merchantability or fitness for a particular purpose. No warranty may be created or extended by sales representatives or written sales materials. The advice and strategies contained herein may not be suitable for your situation. You should consult with a professional where appropriate. Neither the publisher nor author shall be liable for any loss of profit or any other commercial damages, including but not limited to special, incidental, consequential, or other damages.

For general information on our other products and services or for technical support, please contact our Customer Care

Department within the United States at (800) 762-2974, outside the United States at (317) 572-3993 or fax (317) 572-4002.

Wiley also publishes its books in a variety of electronic formats. Some content that appears in print may not be available in electronic formats. For more information about Wiley products, visit our web site at www.wiley.com.

Library of Congress Cataloging-in-Publication Data is available.

ISBN: 978-1-118-99520-4

ISSN: 1042-1122

Preface

This volume is a collection of research papers from the Next Generation Biomaterials and Surface Properties of Biomaterials symposia, which took place during the Materials Science & Technology 2013 Conference & Exhibition (MS&T'13), October 27–31, 2013 at the Palais des Congress, in Montréal, Quebec, Canada.

These symposia focused on several key areas, including biomaterials for tissue engineering, ceramic biomaterials, metallic biomaterials, biomaterials for drug delivery, nanostructured biomaterials, biomedical coatings, and surface modification technologies.

We would like to thank the following symposium organizers for their valuable assistance: Kalpana Katti, North Dakota State University; Mukesh Kumar, Biomet Inc; Kajal Mallick, University of Warwick; Sharmila Mukhopadhyay, Wright State University; Vilupanur Ravi, California State Polytechnic University, Pomona; and Varshni Singh, Louisiana State University. Thanks also to all of the authors, participants, and reviewers of this Ceramic Transactions proceedings issue.

We hope that this issue becomes a useful resource in the area of biomaterials research that not only contributes to the overall advancement of this field but also signifies the growing roles of The American Ceramic Society and its partner materials societies in this rapidly developing field.

SUSMITA BOSE, Washington State University

AMIT BANDYOPADHYAY, Washington State University

ROGER NARAYAN, UNC/NCSU Joint Department of
Biomedical Engineering

BIOACTIVE GLASS-CERAMIC SCAFFOLDS WITH HIGH- STRENGTH FOR ORTHOPEDIC APPLICATIONS

E.A. Aguilar-Reyes, C.A. León-Patiño, E. Villicaña-
Molina

Instituto de Investigaciones Metalúrgicas, Universidad
Michoacana de San Nicolás de Hidalgo, Edificio “U”, Av.
Francisco J. Múgica S/N Ciudad Universitaria, C.P. 58030
Morelia, Michoacán, México

L.-P. Lefebvre

National Research Council Canada (NRC), Boucherville
Research Facilities, 75 de Mortagne Boulevard, Building BOU-
1 Boucherville, Quebec, J4B 6Y4 Canada

ABSTRACT

This study aims to produce 45S5 bioactive glass scaffolds (45% SiO₂-24.5% CaO-24.5% Na₂O-6% P₂O₅) through a novel process of powder technology and polymer foaming, patented by the IMI (Industrial Materials Institute, NRC). Initially, various foaming agent/binder/bioglass powder ratios were proved and the optimal ratio was 0.5/54.5/45.0 in wt. %, respectively. The mixing of the powders was carried out in a shaker-mixer and it was compacted in alumina molds. The samples obtained were submitted to a heat treatment in two stages, the first one, foaming, and the second one, pyrolysis and sintering in the same thermal profile, with the goal of

obtaining scaffolds with mechanical properties and a bioactive response by immersion in SBF appropriated for orthopedic applications. The sintering temperature of scaffolds was 975°C. Then, the scaffolds were machined to obtain uniform cylindrical samples for mechanical testing and cut into tablets of 3 mm in thickness that were immersed in SBF for bioactivity tests for 0, 1, 3, 7, 14, 21 and 28 days. The characterization of scaffolds before immersion in SBF was performed by scanning electron microscopy (SEM) and microtomography (μ CT), also they were tested for compression, and measurement of density and porosity. After immersion the samples were observed with SEM and analyzed by EDS, X-ray diffraction (XRD) and infrared spectroscopy (FT-IR), also the mass variation was estimated. The scaffolds obtained by the experimental method described above, showed a 55 to 65% interconnected porosity and an average compressive strength of 13.78 ± 2.43 MPa, and showed the formation of hydroxyapatite layer after 7 days of immersion in SBF, fulfilling the requirements to be used as a regenerative scaffold. The proposed method of powder technology and polymer foaming, allows controlling the porosity, pore size and compression strength of the scaffolds by varying the ratio foaming agent/binder/bioglass powder and sintering temperature.

INTRODUCTION

The potential of biomaterials for tissue regeneration has been shown *in vitro* and in clinical practice; these materials have been certain compositions of bioactive glasses that offer the ability to adapt to the soft and/or hard tissue. The bioactivity of a material has been associated with the formation of hydroxyapatite crystals in the surface in contact with natural or synthetic body fluids, similar to the inorganic

structure of the bone and it has been shown that bioactive glasses exert a control in the production of osteoblasts on cell cycle.¹ This discovery has stimulated research into the use of bioactive glasses as scaffolds for tissue engineering and has concluded that the bioactive glass 45S5 is the one with the highest potential to be used as three-dimensional matrix (regenerative scaffold) in a large number of human bone components. Recent studies have shown that the ability to regenerate human tissue through the production of hydroxyapatite depends on the porosity of the bioactive glass; the bioactive glass has a higher capacity, if this is more porous.²⁻⁵ Note that this porosity should be interconnected, which is why research continues to study the different ways to produce bioglass foams to obtain characteristics similar to human bone. Currently there are three techniques to produce bioglass foams, the replica technique, technique sacrifice and direct foaming technique.⁶

The main objective of this study is to implement a methodology to obtain bioactive scaffolds from bioglass powders and to examine the relationships between their microstructure and bioactivity. This work is based on the principle that it is possible to obtain controlled reabsorption and dissolution rates of species that promote the regeneration of tissue by manufacturing glasses with structure that mimics trabecular bone structure. The bioactivity of the bioglass scaffolds will be monitored by evaluating the *in vitro* formation of calcium phosphate layer on their surface.

METHODOLOGY

Preparation of 45S5 Bioactive Glass

45S5 glass was prepared by the traditional melting-quenching method of a mixture of high purity powders of SiO_2 , Na_2CO_3 , CaO and P_2O_5 (Sigma-Aldrich, St. Louis, MO, USA), prepared stoichiometrically to obtain the final composition of $24.5\text{Na}_2\text{O}-24.5\text{CaO}-6\text{P}_2\text{O}_5-45\text{SiO}_2$ (wt. %).

Fabrication of 45S5 Bioglass Scaffolds

Scaffolds of 45S5 bioactive glass were produced by the combined method of powder technology and foaming of polymers, described in [7], since it is a novel method, easy to handle, and does not generate high costs. The glass powder was mixed with a phenolic resin (Varcum 29217, Durez Corporation, Niagara Falls, NY, USA) and a foaming agent (p-toluenesulfonyl hydrazide or TSH, Sigma-Aldrich, St. Louis, MO, USA) in the ratio 45/54.5/0.5 in wt. %, respectively. The powder mixture was poured into a SS mold for foaming, during this process the binder was melted to form a suspension with the glass particles and then the foaming agent decomposed to generate an expanding gas. After foaming, the resulting material was a phenolic resin foam loaded with 45S5 bioactive glass particles. The foams were machined into small cylinders of 18 mm in diameter and 20-30 mm in length, and then heat-treated at 500°C for 2 h to burn out the binder and sintered in air at 975°C for 1 h to consolidate the material.

Bioactivity Tests

The cylindrical scaffolds were cut into discs with dimensions of 10 mm in diameter and 3 mm in thickness, taking precautions to have no contamination. The discs were immersed in simulated body fluid (SBF) following the protocol published by Kokubo *et al.*⁸. Various times were selected for immersion in SBF, 1, 3, 7, 14, 21 and 28 days. The immersed discs were maintained at 37°C in polyethylene vials under sterile conditions in a cell culture

room. After each immersion time, the sample was removed from the fluid and dried in an oven at 90 °C for 24 h and subsequently was placed in a desiccator.

Characterization of 45S5 Bioglass Scaffolds

The microstructure of the scaffolds was characterized with a JSM-6100 JEOL scanning electron microscope (JEOL, Tokyo, Japan) and a X-Tek HMXST 225 X-ray μ CT (Nikon Metrology, Tring, UK). Scaffolds, before and after bioactivity tests, were characterized by X-ray diffraction (Bruker AXS D8 Discover X-Ray Diffractometer) to determine the crystalline phases after sintering and the evolution of the hydroxyapatite layer, respectively. The acquisition data was carried out in the range of 20-90° 2 θ using a 0.04° step and 2 s/step. The specific surface area, which is an important feature that influences aspects such as reaction kinetics and it is also required to calculate the SBF volume for immersion of each disk, was measured in a surface area analyzer HORJBA-SA 9600 series. The gas used for the analysis was nitrogen and the value for the bioglass scaffolds was 0.13 m²/g. Functional groups of bioactive glass and hydroxy apatite phases were determined by infrared spectroscopy in 45S5 bioactive glass scaffolds before and after immersion in SBF. Each spectrum comprises 32 independent scans in transmittance, measured at a spectral resolution of 1 cm⁻¹ within the 4,000 - 400 cm⁻¹ range, in a Bruker Tensor 27 FT-IR Spectrometer (Bruker, Germany).

For scaffold unconfined compression tests, six cylindrical samples (10 mm in diameter and 5 - 9 mm in length), selected randomly, were tested in a universal machine MTS with a load cell of 5 KN. The cross-head loading speed was set at 2.5mm/min.

RESULTS AND DISCUSSION

The scaffolds had porosity between 55 – 65% and the volume decreased about 25% of the initial volume after pyrolysis and sintering.

The SEM micrographs of the sintered scaffolds are shown in [Figure 1](#), it can be seen that the porous structure is uniform throughout the sample and the porosity is interconnected with pore size in the range of 50 – 600 μm .

[Figure 1](#). SEM micrographs of porous structure of 45S5 scaffolds sintered at 975°C at various magnifications: (a) 15x, (b) 200x, and (c) 400x.

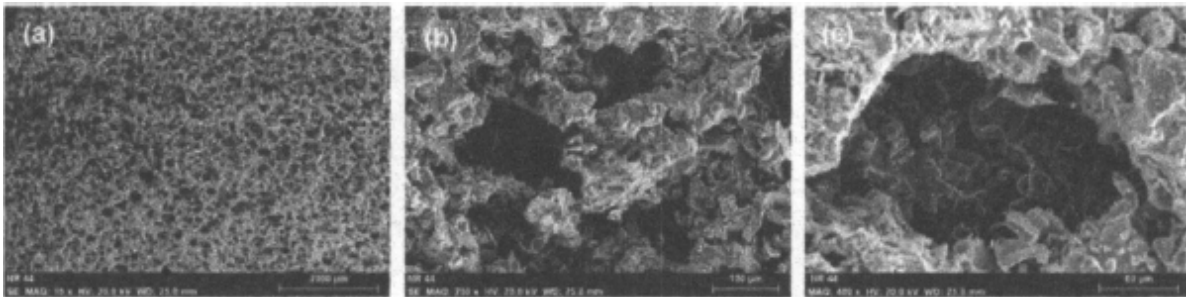


[Figure 2](#) shows 2-D and 3-D microtomography (μCT) images obtained from sintered scaffolds. It can be observed a uniform and interconnected porosity as well as the thickness of the struts in the scaffolds. The graph represents the pore size distribution, on the left side is the volumetric frequency up to 10.5% for a pore size 250 μm and on the right side is the a volumetric cumulative frequency up to 100%. The behavior is cuasimodal and the pore size distribution is in the range of required parameters (50-600 μm) for a regenerative scaffolds.

[Figure 2](#). Pore size distribution and microtomography (μCT) of scaffold sintered at 975°C.

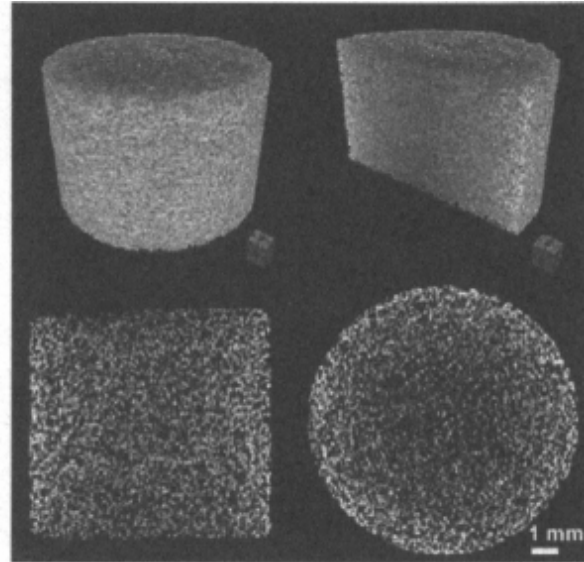
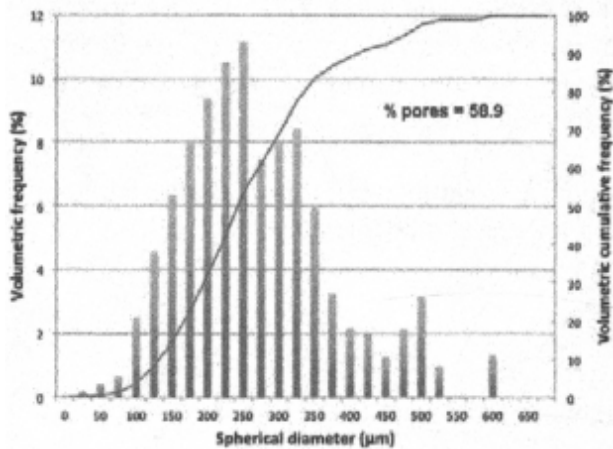


[Figure 3](#) shows the XRD pattern of 45S5 bioactive glass and foams made at 975°C. The spectrum of the powder showed that the initial powder for producing foams is amorphous. However foams spectra show peaks representative of the crystalline phases: $\text{Na}_6\text{Ca}_3\text{Si}_6\text{O}_{18}$ (JCPDS 77-2189) y $\text{Na}_2\text{Ca}_4(\text{PO}_4\text{SiO}_4)$ (JCPDS 29-1193), the same have been identified by other investigators in previous studies of sintered bioactive glasses of the same composition⁹⁻¹¹ This clearly indicates that a process of crystallization is present during sintering of foams.

[Figure 3](#). XRD spectra of 45S5 bioglass powder and bioglass scaffold sintered at 975°C.

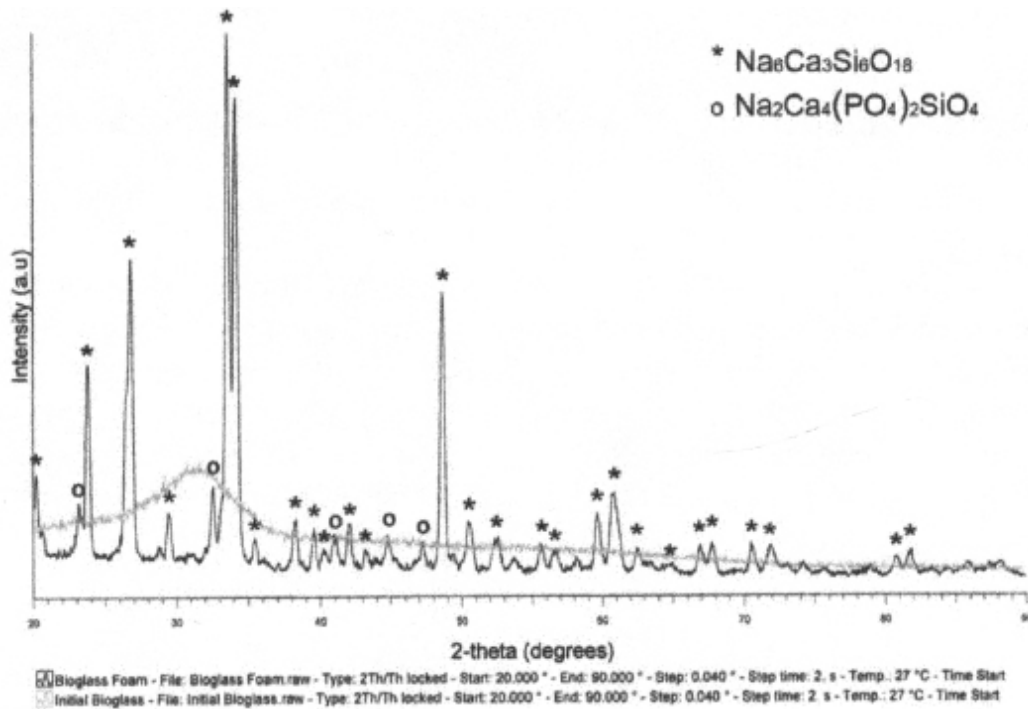


[Figure 4](#) shows the formation of hydroxyapatite layer as a function of immersion time on the surface of bioglass sintered structure. It can be observed that hydroxyapatite tends to form agglomerates of spherical nanoparticles as of 7 days of immersion in SBF. The presence of hydroxyapatite phase was also confirmed by XRD and FT-IR analyses.

[Figure 4](#). SEM micrographs showing the development of the hydroxyapatite layer on the surface of bioglass scaffolds at various immersion times in SBF: (a) 0, (b) 1, (c) 3, (d) 7, (e) 21, and (f) 28 days.

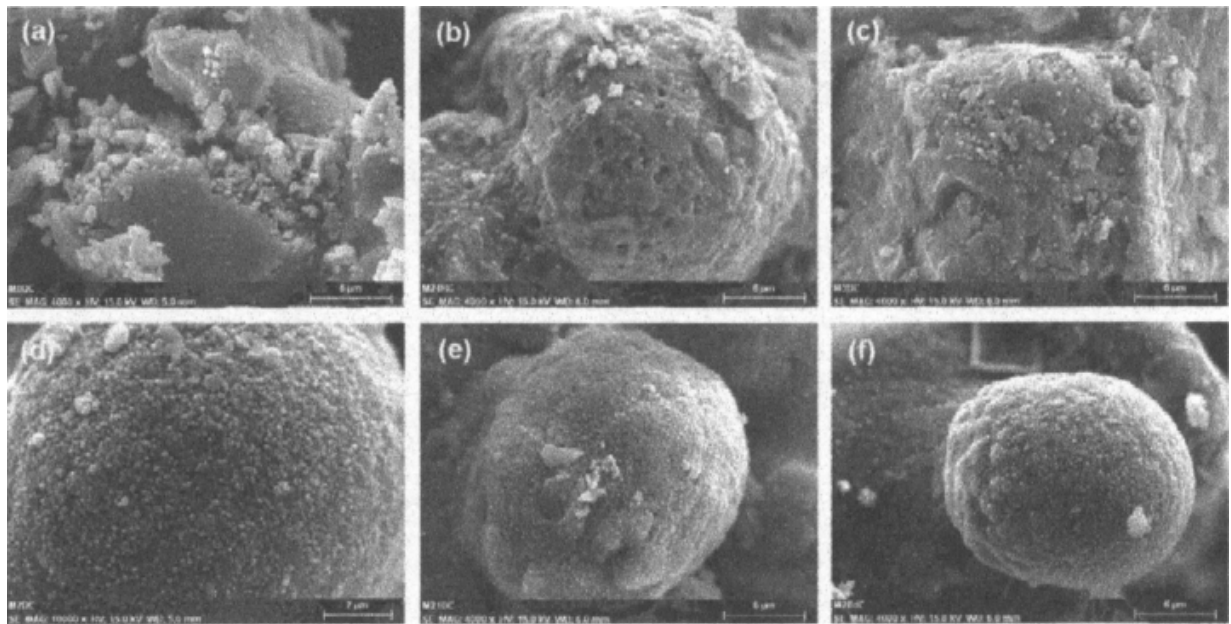
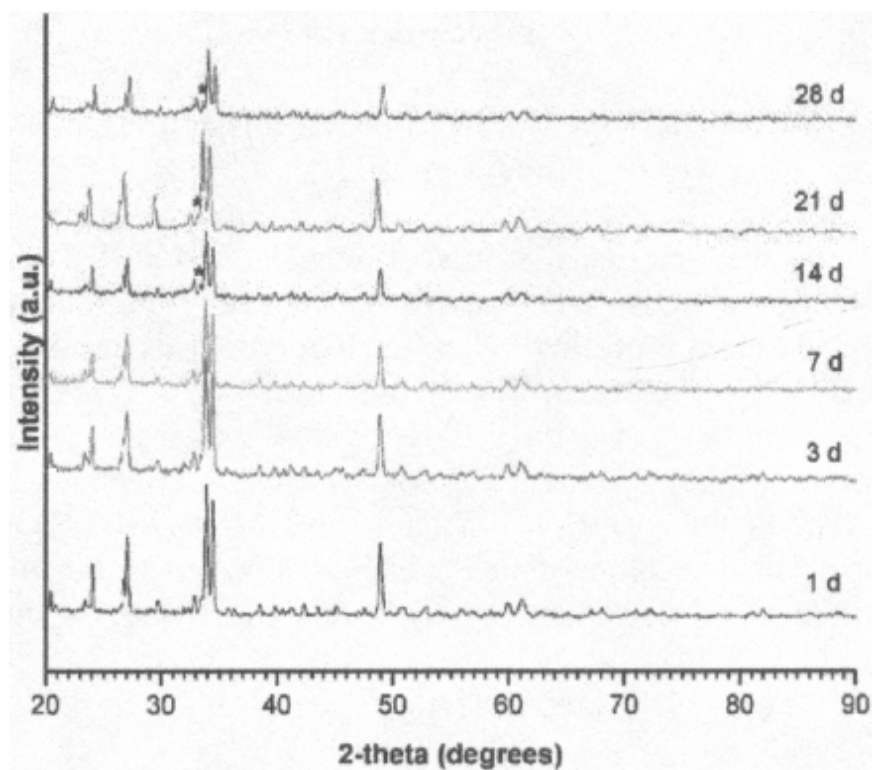


[Figure 5](#) shows the XRD patterns for the scaffolds at various times of immersion in simulated body fluid. It can be observed the presence of the peak of the hydroxyapatite phase, which increases in intensity as a function of immersion time while the intensity of the reflections corresponding to the crystalline phases in the scaffold developed after sintering decrease.

[Figure 5](#). X ray spectra of bioglass scaffold sintered at 975°C and immersed in SBF for various times.



The IR spectra for the scaffold sintered at 975°C, before and after immersion in SBF for 14 days, are shown in [Figure 6](#). A typical HA phase shows bands in FTIR spectrum in (3600, 3569, 3578, 3448 and 633) cm^{-1} for OH^- groups, bands (474, 571, 601, 692, 1032 \approx 1087, 1092, 1040) cm^{-1} corresponding to groups PO_4^{3-} and bands (870, 1420 and 1480) cm^{-1} if the sample contains CO_3^{2-} groups¹². Several of these bands are present in the sample subjected to 14 days of immersion in SBF, as can be observed in [Figure 6](#) (3746, 3409, 1483, 1450, 1038, 692, 630, 572 cm^{-1}). This means that the obtained peaks are representative of a phase very close to a stoichiometric HA.

[Figure 6](#). Infrared spectroscopy analyses for bioglass scaffolds before and after immersion for 14 days in SBF.